

# Accumulation rates in Dronning Maud Land, Antarctica, as revealed by dielectric-profiling measurements of shallow firn cores

H. OERTER,<sup>1</sup> F. WILHELMS,<sup>1</sup> F. JUNG-ROTHENHÄUSLER,<sup>1</sup> F. GÖKTAS,<sup>1</sup> H. MILLER,<sup>1</sup> W. GRAF,<sup>2</sup> S. SOMMER<sup>3</sup>

<sup>1</sup>Alfred-Wegener-Institut für Polar- und Meeresforschung, Postfach 120161, D-27515 Bremerhaven, Germany

<sup>2</sup>GSF-Forschungszentrum für Umwelt- und Gesundheit München, D-85764 Neuherberg, Germany

<sup>3</sup>Physikalisches Institut, Universität Bern, CH-3012 Bern, Switzerland

**ABSTRACT.** The European Programme for Ice Coring in Antarctica includes a comprehensive pre-site survey on the inland ice plateau of Dronning Maud Land, Antarctica. The German glaciological programme during the 1997/98 field season was carried out along a 1200 km traverse on Amundsenisen and involved sampling the snow cover in pits and by shallow firn cores. This paper focuses on the accumulation studies. The cores were dated by dielectric-profiling and continuous-flow analysis. Distinct volcanogenic peaks and seasonal signals in the profiles served to establish a depth time-scale. The eruptions of Krakatoa, Tambora, an unknown volcano, Kuwae and El Chichon are well-documented in the ice. Variations of the accumulation rates over different times were inferred from the depth time-scales. A composite record of accumulation rates for the last 200 years was produced by stacking 12 annually resolved records. According to this, accumulation rates decreased in the 19th century and increased in the 20th century. The recent values are by no means extraordinary, as they do not exceed the values at the beginning of the 19th century. Variations in accumulation rates are most probably linked to temperature variations indicated in  $\delta^{18}\text{O}$  records from Amundsenisen.

## INTRODUCTION

The European Project for Ice Coring in Antarctica (EPICA) focuses on two deep ice-core drillings in two regions within Antarctica, the Dome Concordia (Dome C) area in the Indian/Pacific sector and Dronning Maud Land (DML) in the Atlantic sector of Antarctica. The inland ice of DML is still a rather unexplored part of the Antarctic ice sheet. Therefore an intensive pre-site survey programme was set up, comprising ice-thickness measurements by airborne radio-echo-sounding surveys, ice-flow measurements by global positioning system (GPS) survey and glaciological investigations on shallow firn cores and 100 m ice cores. The core studies will reveal the accumulation distribution across Amundsenisen and the accumulation and climate history during the last millennium. Norway, Sweden, The Netherlands, the United Kingdom and Germany (Oerter and others, 1999) have been engaged in traverse work and airborne surveys since the 1995/96 field season. This paper describes the German traverse work in 1997/98 starting at Neumayer station on the coast and crossing Amundsenisen to the plateau of the inland ice.

## FIELDWORK

The area of the EPICA pre-site survey in DML is Amundsenisen, East Antarctica (Fig. 1). It includes the region between 72° S and 78° S, and between 15° W and 20° E. In the 1997/98 field season, a ground traverse was carried out between 5 December 1997 and 2 February 1998, from Neumayer, the

German wintering-over base, across Ritscherflya and up to the inland ice plateau east of Heimefrontfjella. The traverse route on Amundsenisen was approximately 1200 km. All measuring sites were identified as DMLxx (DML for Dronning Maud Land) with xx being a running number for the sites visited since the 1995/96 season (Fig. 1, Table 1). The sites

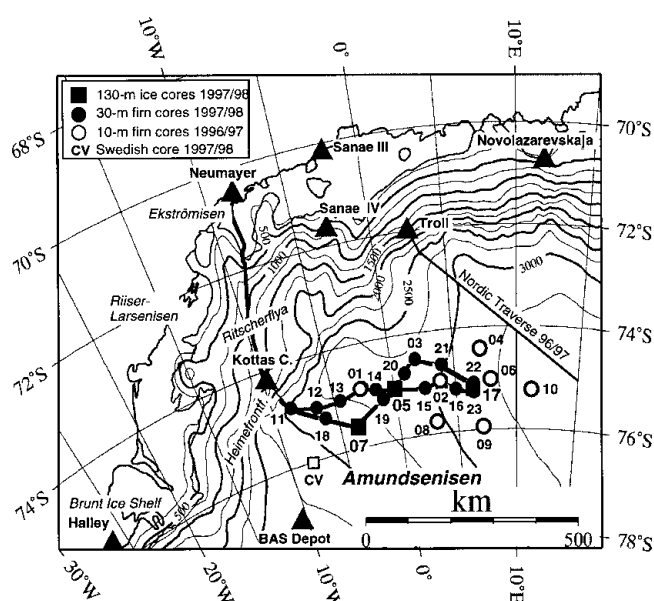


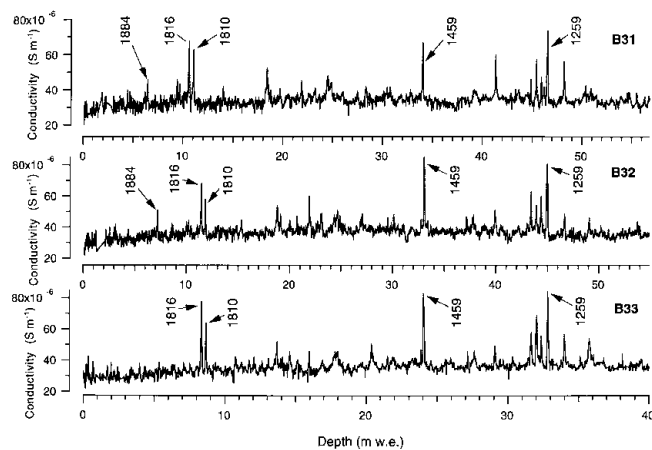
Fig. 1. Dronning Maud Land showing the AWI traverse route 1997/98 and drill locations. Elevation data based on ERS-1 altimetry (courtesy of J. Bamber, University of Bristol).

Table 1. Coordinates for drill locations on Ekströmisen, Ritscherflya and Amundsenisen during the 1997/98 field season (Fig. 1). The WGS84 coordinates were converted with the OSU91A model to orthometric heights (<http://gibs.leibniz-ifa.de>). Also shown are firn temperatures measured in the boreholes at 10 m depth

Locality	Core label	Date	Latitude	Longitude	Elevation		10 m temp.
					WGS84	orthom.	
		dd/mm/yy			m	m a.s.l.	°C
Pegelfeld Süd	FB9801	04/12/1997	70°42.40' S	8°25.6' W		45	-17.0
Kottas camp	FB9802	11-12/12/1997	74°12.30' S	9°44.50' W	1451	1439	-25.2
DML02	DML9602	01/02/1996	74°58.10' S	3°55.12' W	3027	3014	-44.4
DML03	FB9809	02/01/1997	74°29.95' S	1°57.65' E	2855	2843	-42.2
DML05	B32	25-29/12/1997	75°00.14' S	0°00.42' E	2892	2882	-44.5
About 500 m E of DML05	FB9806	29/12/1997	75°00.16' S	0°01.36' E		2880	
About 1000 m NE of DML05	FB9807	30/12/1997	74°59.82' S	0°02.17' E		2880	
DML07	B31	19-21/12/1997	75°34.89' S	3°25.82' W	2680	2669	-44.3
DML11	FB9803	15/12/1997	74°51.28' S	8°29.82' W		2600	-37.1
DML12	FB9817	21/01/1998	75°00.04' S	6°29.90' W		2680	-40.2
DML13	FB9816	19/01/1998	75°00.00' S	4°29.78' W		2740	-42.3
DML14	FB9815	17/01/1998	74°56.95' S	1°29.67' W		2840	
DML15	B9814	14/01/1998	75°05.02' S	2°30.06' E		2970	-45.0
DML16	FB9813	12/01/1998	75°10.04' S	5°00.20' E		3100	-45.5
DML17	B33	7-10/1/1998	75°10.02' S	6°29.91' E		3160	-46.1
DML18	FB9804	17/12/1997	75°15.02' S	6°00.00' W		2630	-40.5
DML19	FB9805	23/12/1997	75°10.04' S	0°59.70' W		2840	-43.4
DML20	FB9808	31/12/1997	74°45.04' S	0°59.99' E		2860	-43.1
DML21	FB9810	04/01/1998	74°40.03' S	4°00.10' E		2980	-44.0
DML22	FB9811	06/01/1998	75°05.04' S	6°30.00' E		3160	
DML23	FB9812	11/01/1998	75°15.05' S	6°30.10' E		3160	-45.8

DML11–DML23 were first visited in 1997/98. The traverse programme in 1997/98 included drilling 15 firn cores at 12 locations to a depth of 30–42 m, and three ice cores 115–150 m deep. The aim of the drilling work was to reach at least the AD1810 layer which is strongly marked by the eruption of an unknown volcano in 1809 and provides, together with the eruption of Tambora in 1815, a common time marker for dating the cores. The drilling was complemented by snow-pit sampling to ensure proper representation of the near-surface layers, because core quality is usually reduced in the uppermost 2 m. The firn cores were logged and packed at the drilling sites and then flown to Neumayer station. The

cores were labelled FB98xx with xx being a running number from 03 to 17 for the cores on Amundsenisen, and 01 and 02 for a core adjacent to Neumayer station and one at the old Kottas field camp, respectively (Table 1). A field laboratory was established at Neumayer, using an old ventilation tunnel connected to the base approximately 5 m under the snow surface. The mean air temperature in the tunnel was  $-10 \pm 2^\circ\text{C}$ . Measuring devices were set up for the combined dielectric profiling (DEP) of the cores (Wilhelms and others, 1998) and density measurements by gamma-ray attenuation (Gerland and others, 1999) as well as for electric-conductivity measurements (ECM; Hammer, 1980). Facilities for cutting the cores and sub-sampling for further analysis were also available. Another small laboratory on the surface contained facilities for continuous-flow analysis (CFA; Sigg and others, 1994). During the field season, all firn cores were analysed with respect to dielectric properties (DEP) and density, 10 cores were measured by ECM and seven cores, including the three long ones, by CFA. The cores and cut samples were shipped back at the end of the field season for cold storage at the Alfred Wegener Institute (AWI) in Bremerhaven.



### DATING THE FIRN CORES

Dating the firn cores was done using the DEP and CFA data. The DEP method has been described by Moore and Paren (1987) and Wilhelms and others (1998). The DEP data presented here were taken at 250 kHz, in 5 mm increments with a 10 mm long measuring electrode. To account for density variations in the upper firn section, the DEP data were corrected with a complex continuation of the Looyenga (1965) mixing model, as suggested by Glen and Paren (1975). Concentrations of sodium, calcium, ammonium, hydrogen peroxide and the electrolytical conductivity were measured with a CFA technique (Sigg and others, 1994). For initial dating,

Fig. 2. DEP conductivity profiles of ice cores B31, B32 and B33. The conductivity was corrected for density fluctuations using Looyenga's (1965) mixing model. The main peaks used for dating the cores are marked (Table 2). The depth axes are given in m.w.e. and are scaled so that the 1259 peaks correspond graphically for the three cores.

Table 2. Volcanic events identified in the ice cores

Volcano	Date of eruption/ deposition	Depth of the horizons at		
		DML07 (core B31) m w.e.	DML05 (core B32) m w.e.	DML17 (core B33) m w.e.
Krakatoa	1883/84	6.47	7.22	5.44
Tambora	1815/16	10.62	11.46	8.36
Kuwaë	1458/59	34.01	33.04	24.00
El Chichon	1258/59	46.53	45.00	32.80

some distinct peaks, displayed in the DEP profiles (Fig. 2), were assigned to volcanic events described in the literature to obtain long-term accumulation values before resolving the details of the last 200 years. The most prominent peaks found in all three deeper cores are listed in Table 2. Unfortunately, no nss-sulfate concentrations, which could prove the volcanic origin of the DEP peaks, have yet been determined. Two periods are very significant for dating purposes; 1810 to 1816 with the twin peak of an unknown volcano and Tambora; and 1259 to 1287 with a pattern of four peaks. Another event occurs in all three cores between these two periods at comparable depths. In the following, the horizons used for dating are described in more detail.

The deepest and largest peak in the group of the four marks the 1259 horizon, according to Langway and others (1988). Delmas and others (1992) assumed that this peak was connected with an early eruption of El Chichon, Mexico, based on the work of Palais and others (1990). This assumption is confirmed by Palais and others (1992). The pattern with four peaks is described by Delmas and others (1992) and Langway and others (1994, 1995) who dated peaks in cores from Byrd station and South Pole nearly equal to the years 1259/1259, 1270/1269, 1278/1277 and 1287/1285, respectively. Moore and others (1991) show a DEP conductivity profile of a core from Mizuho plateau with only one distinct peak, assigned to 1259. At Dome Fuji, four peaks are also reported (Dome F Deep Coring Group, 1998).

The single event documented in the three cores at comparable relative depths to the 1259 peak was assigned to 1459. This event is not as well-documented in the literature as the 1259 event. Cole-Dai and others (1997) ascribed a similar peak, in a core from Siple station, to the eruption of Kuwaë. Delmas and others (1992) mention a volcanic horizon for 1450 at South Pole, Langway and others (1995) for 1464 at Byrd station and for 1450 at South Pole, but they conclude that the deposition year most probably was 1459 as revealed by a Greenland ice core at Crête. The Dome F Deep Coring Group (1998) do not mention a peak then and Moore and others (1991) follow Legrand and Kirchner (1990) and assign the corresponding peak to 1460.

The twin peaks from 1810 and 1816 are displayed in all cores from Amundsenisen. These peaks are well-dated for Antarctic ice cores and reported by Langway and others (1995) for Byrd station and South Pole, Delmas and others (1992) for South Pole, Cole-Dai and others (1997) for Siple station and Moore and others (1991) for Mizuho plateau. They were identified without doubt for the ice cores B31, B32 and B33 as well as for the firn cores FB9804–FB9817. The firn cores FB9801 (Neumayer station, Pegelfeld Süd), FB9802 (Kottas camp) and FB9803 (DML11) do not reach

this date due to higher accumulation rates. How well they are represented in the different DEP profiles can be seen from Figure 3.

Figure 3 displays the whole set of DEP profiles for the period since 1810. There are several other signals in the DEP profiles which helped to synchronize the dating of the cores. However, they are not as evident as the 1816 and 1810 peaks. Nine peaks were selected at core B32 (Fig. 3, 1–9) which can be correlated with peaks in the other cores (marked by asterisks). From 1832 to 1836, two peaks are displayed (6 and 7) at core B32 and in several of the other cores. One of them could correspond to a peak present in the snow cover at Byrd station (Langway and others, 1995), at South Pole (Delmas and others, 1992; Langway and others, 1995), at Dyer Plateau (Cole-Dai and others, 1997), at Siple station (Cole-Dai and others, 1997) and at Mizuho plateau (Moore and others, 1991). Delmas and others (1992) dated this peak in the nss-sulfate profile to the year  $1836 \pm 2$  and assigned it to the 1835 eruption of Cosiguina in Nicaragua. It is very likely that peak 6 corresponds to this eruption.

The eruptions of Krakatoa in 1883 and Tarawera in 1886 (Newhall and Self, 1982) belong to the strongest during the past 200 years, after the 1815 eruption of Tambora and that of the unknown volcano in 1809. The Krakatoa eruption was detected in the 1884 layer of nss-sulfate profiles at Byrd sta-

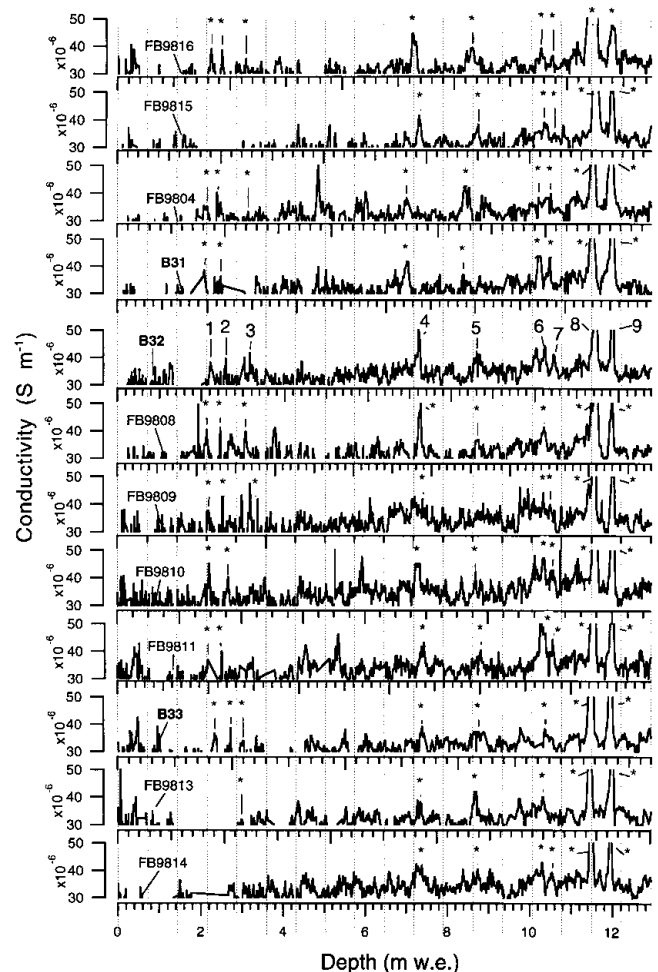


Fig. 3. DEP profiles of firn cores from DML. The depth axes are given in m w.e. and are scaled so that the 1810 peaks correspond graphically for the 12 cores. Nine peaks are labelled at core B32 (1–9) and are detectable also in the other cores (marked by asterisks).

tion (Langway and others, 1995), at South Pole (Delmas and others, 1992; Langway and others, 1995) and at Mizuho plateau (Moore and others, 1991). Isaksson and others (1996, 1999) used this time marker for dating firn cores in DML. A corresponding peak was also found (peak 4 at B32); it is pronounced in most of the cores, but very weak in cores FB9809 and FB9804.

The 1963 eruption of Agung (peak 1 at B32) was not clearly detectable in each of the cores, partly due to bad core quality in this depth interval. There are two more peaks (2 and 3) which coincide with the years  $1959 \pm 1$  and  $1952 \pm 1$  in the dated cores. The source of these peaks is unclear.

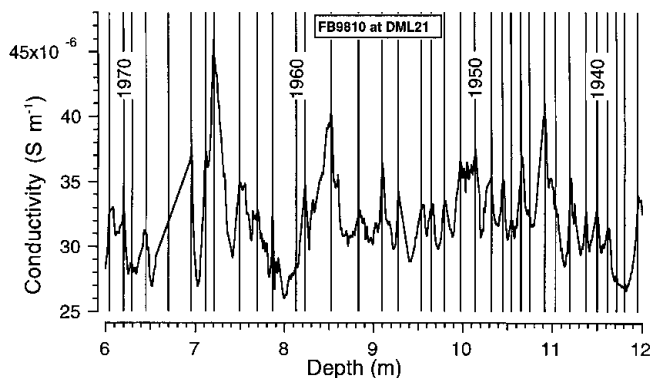


Fig. 4. DEP profile of firn core FB9810 with density correction after Looyenga (1965) and deduced annual layering.

### Annual layer counting

The profiles of sodium, calcium and ammonium concentration, as well as the DEP profiles, show very regular annual fluctuations (Fig. 4). While enhanced sea-salt concentrations during winter (Wagenbach and others, 1998) cause the sodium and calcium peaks, the seasonality in the ammonium record is not yet understood. Variations in the DEP profiles seem to be due to higher ion concentrations during the summer months (Wilhelms, 1996). As DEP measurements are, in contrast to the CFA results, available for all cores, these profiles were used for year-to-year dating with the common reference horizons being 1816 and 1810. The peaks in the DEP profiles (the summer horizons) were used for defining annual layers. Thus they mark the beginning or end of a calendar year. DEP values from pieces with core-catcher damage, or around breaks, were rigorously removed from the datasets. Sometimes missing DEP data could be supplemented with ECM data. For some small, damaged, core pieces neither DEP nor ECM data are available. In such cases, annual layers were introduced by linear interpolation using mean accumulation rates since 1810. Annually resolved depth time-scales, with the 1810 horizon as a common fixed point, were established for all cores and used to calculate chronologies of annual accumulation rates and annual  $\delta^{18}\text{O}$  values (five cores only so far). Examples of the annual variation of the electric conductivity determined by DEP and the deduced annual layers are shown in Figure 4. The counting of annual layers is not possible without some ambiguities and can only be improved by using known reference horizons. The seven DEP peaks since 1816, marked in the profile of core B32 (Fig. 4) and not used for dating, appear in the cores at slightly different dates. This time shift can be used as a

measure of the dating error. Deposition dates and their uncertainties for peaks 1–7 are  $1965 \pm 1.2$ ,  $1959 \pm 1.1$ ,  $1952 \pm 1.1$ ,  $1884 \pm 1.0$ ,  $1862 \pm 2.1$ ,  $1835 \pm 1.3$ ,  $1832 \pm 1.7$ , respectively. Thus we assume that the annual-layer dating from 1810 to 1998 is accurate within  $\pm 2$  years.

## RESULTS AND DISCUSSION

Accumulation rates were calculated using the dating procedures described above and the firn or ice density from gamma-ray attenuation profiles (see Gerland and others (1999) and Wilhelms (1996) for the method used), which were also determined in the field. Four datasets of accumulation rates are now available. The snow-pit data contain the most recent accumulation rates during the last ten years, the 10 m firn cores from the 1995–97 seasons, dated mainly by tritium and DEP (Oerter and others, 1999), covered a period of up to 100 years, the 30 m firn cores from the 1997/98 season a period of 200 years, and the three ice cores to medium depths revealed the accumulation history back to 1259 (Table 3).

Table 3. Long-term accumulation rates on Amundsenisen deduced from volcanic events in the ice cores (see Table 2)

Time interval	Accumulation rates at		
	DML07 (core B31)	DML05 (core B32)	DML17 (core B33)
	kg m <sup>-2</sup> a <sup>-1</sup>	kg m <sup>-2</sup> a <sup>-1</sup>	kg m <sup>-2</sup> a <sup>-1</sup>
1259–1459	62.6	59.8	44.0
1459–1816	65.5	60.4	43.8
1816–1997	58.4	63.0	45.9

### Accumulation history during the last 700 years

#### 1259 to present

Mean values of the accumulation rates in different time spans can be derived directly from the depth of the volcanic horizons given in Table 2. The accuracy of these values is limited by the uncertainty of the dating ( $\pm 1$  year), by the accuracy of the depth scale and by the error of the density values which is in the order of 1%. For example, the accuracy of the 100 year mean-accumulation rate is in the order of 2%.

For 1259–1997, the mean accumulation rates at DML07 (ice core B31), DML05 (core B32) and DML17 (core B33) are 63.0, 60.9 and 44.4 kg m<sup>-2</sup> a<sup>-1</sup>, respectively. For 1459–1997 the mean values are less than 1% different from these values.

However, from 1816–1997, after a 550 year period of nearly constant values at the three sites (Table 3), the accumulation history was different. At DML07, on the southwestern slope, the accumulation rate decreased by about 10%. In contrast, along the ice divide (running east–west), at both DML17 and DML05 the mean values increased by about 5%.

#### 1800 to present

The annually resolved accumulation rates calculated for the last two centuries at 10 sites are shown in Figure 5. The interannual variability of the accumulation rate is high. It is given in Table 4 as a standard deviation of the annual mean values for 1801–1997 corresponding to a percentage between

Table 4. Firn cores and snow pits sampled in 1997/98. The table shows mean accumulation rates and the scatter ( $1\sigma$ ) of the annual values for the given periods. Dating of the cores from 1997/98 is based on DEP profiles, the snow pits were dated using stable isotopes. For DML02, DML03, DML05 and DML07 the results of older cores (Oerter and others, 1999) have also been added

Locality	Core/pit label	Depth to m	Time interval	Accumulation rate $\text{kg m}^{-2} \text{a}^{-1}$
Neumayer, Pegelfeld Süd	FB9801	27.02	1948–1997	$317 \pm 107$
Kottas	FB9802	26.43	1881–1997	$129 \pm 38$
Kottas	FBK9601	10.66	1962–1995	$125 \pm 16$
DML02	DML9602	10.79	1919–1995	$57 \pm 14$
DML02	SS9813	0.47	1995–1997	$51 \pm 17$
DML03	DML9703	11.56	1941–1996	$91 \pm 29$
DML03	FB9809	33.01	1801–1997	$89 \pm 29$
DML03	SS9807	1.00	1994–1997	$89 \pm 25$
DML05	B32	25.44	1801–1997	$62 \pm 21$
DML05	DML9705	11.16	1930–1996	$71 \pm 21$
DML05	SS9805	2.68	1985–1997	$71 \pm 19$
500 m E DML05	FB9806	23.80	1816–1997	62
1000 m NE DML05	FB9807	24.20	1816–1997	67
DML07	B31	24.92	1801–1997	$59 \pm 24$
DML07	DML9707	12.13	1908–1996	$57 \pm 16$
DML07	SS9803	2.46	1985–1997	$62 \pm 19$
DML11	SS9801	2.04	1989–1997	$76 \pm 18$
DML12	FB9817	23.00	1816–1998	62
DML12	SS9818	1.85	1989–1997	$68 \pm 17$
DML13	FB9816	19.73	1800–1997	$47 \pm 17$
DML13	SS9817	1.77	1991–1997	$80 \pm 20$
DML14	FB9815	25.77	1801–1997	$53 \pm 19$
DML14	SS9815	1.95	1990–1997	$81 \pm 37$
DML15	FB9814	25.77	1801–1997	$64 \pm 21$
DML15	SS9814	2.07	1988–1997	$71 \pm 18$
DML16	FB9813	19.30	1816–1997	48
DML16	SS9812	2.01	1988–1997	$70 \pm 22$
DML17	B33	19.57	1801–1997	$47 \pm 16$
DML17	SS9810	1.72	1989–1997	$63 \pm 17$
DML18	FB9804	20.57	1801–1997	$50 \pm 16$
DML18	SS9802	1.77	1988–1997	$55 \pm 15$
DML19	FB9805	18.40	1810–1997	44
DML19	SS9804	2.25	1988–1997	$78 \pm 24$
DML20	FB9808	26.77	1801–1997	$68 \pm 22$
DML20	SS9806	1.71	1992–1997	$97 \pm 19$
DML21	FB9810	32.18	1801–1997	$86 \pm 29$
DML21	SS9808	1.88	1990–1997	$83 \pm 23$
DML22	FB9811	23.45	1801–1997	$58 \pm 16$
DML22	SS9809	0.86	1994–1997	$74 \pm 17$
DML23	FB9812	16.30	1816–1997	38
DML23	SS9811	1.05	1993–1997	$69 \pm 25$

32% and 36% (except at DML07). An even higher variability, of 40%, is found at DML07 (B31) in the southwestern part of the investigation area.

The time series were smoothed using a Gaussian low-pass filter over 11 years to account for the high-frequency deposition noise (thick line in Fig. 5). The individual time series were stacked to produce a composite record of accumulation rates for Amundsenisen. The smoothed time series reveal a statistically significant increase for DML03 (core FB9809), DML20 (core FB9808), DML05 (core B32) and DML15 (core FB9814), and a negative trend over the 200 year period since 1800 for the DML18 (core FB9804). All other cores do not show a trend over the 200 year period.

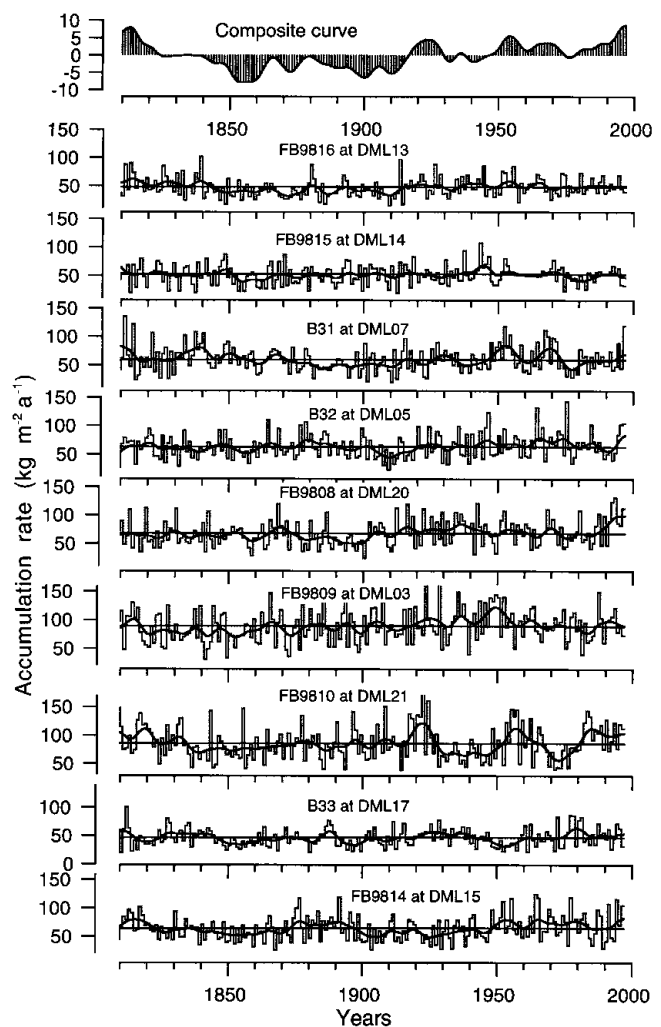


Fig. 5. Annually resolved time series of accumulation rates at nine locations on Amundsenisen. The thick line was created by smoothing the records with a Gaussian low-pass filter over 11 years. The composite record is shown on top as deviations from the mean value (it includes also the records from cores FB9804, FB9811 and FB9813, which are not shown).

Changes of accumulation rates of regional relevance for Amundsenisen can be expected from the stacked series.

According to the stacked series, the accumulation rate,  $A$ , decreased in the 19th and increased in 20th century, with a turn of the trend around 1905. Linear regression analysis results in  $dA/dt = -0.124 \pm 0.021 \text{ kg m}^{-2} \text{ a}^{-2}$  ( $r = -0.50$ ) and  $0.068 \pm 0.024 \text{ kg m}^{-2} \text{ a}^{-2}$  ( $r = 0.20$ ), respectively. The 20th century started with minimum accumulation rates and ends with values no higher than at the beginning of the 19th century. Similar trends are found for the stable isotopes, as will be shown later (Fig. 7).

### Spatial distribution of accumulation

The local variability of the snow cover and of the accumulation rates can be assessed by comparing the results of cores recovered close together. At DML03, DML05 and DML07, accumulation rates were determined using different cores and pits (Table 4). Here, we compare only the means over the period 1960–96, not the fluctuations in the time series. This period was selected because the cores taken in 1997 were dated by tritium profiles back to 1960. At all locations the

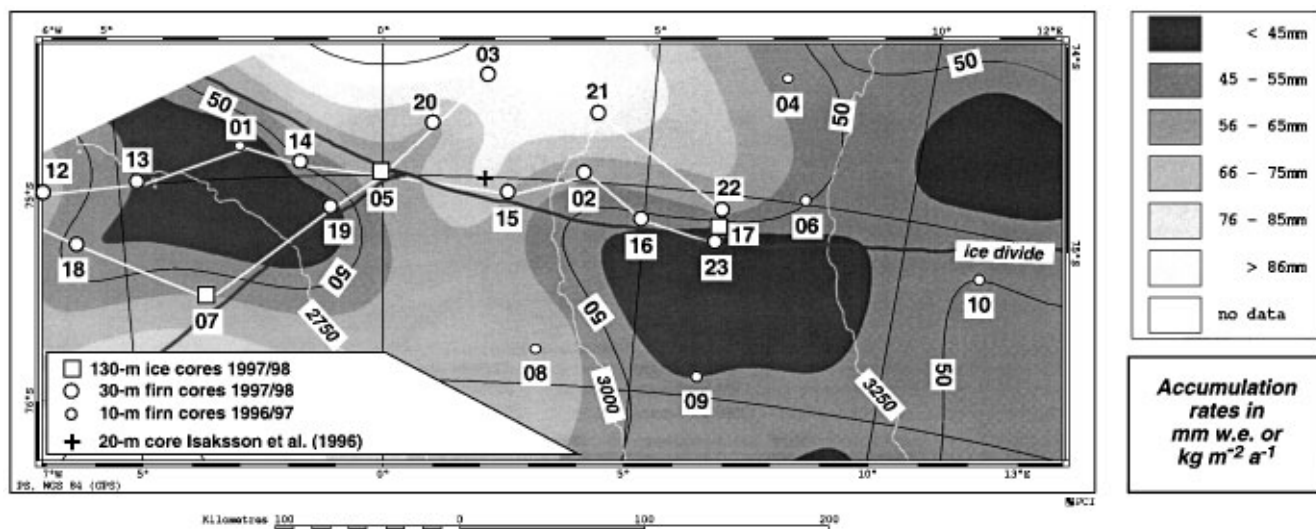


Fig. 6. Accumulation rates on Amundsenisen in the area covered by the firn cores (numbered points, cf. Fig. 1) drilled by AWI between 1995 and 1998. The thick white line shows the German traverse route in 1997/98. The cross marks the location of a 20 m firn core by Isaksson and others (1996). The white lines are contour lines (cf. Fig. 1), the thin black line is the isoline for an accumulation rate of  $50 \text{ kg m}^{-2} \text{ a}^{-1}$ . The ice divides crossing the area under investigation are also indicated.

values agree well: at DML03, the location with the highest accumulation rate, the values from the two cores DML9703 ( $89.5 \text{ kg m}^{-2} \text{ a}^{-1}$ ) and FB9809 ( $90 \text{ kg m}^{-2} \text{ a}^{-1}$ ) are within the accuracy limit. At DML05, the accumulation rates determined with core DML9705 ( $70.1 \text{ kg m}^{-2} \text{ a}^{-1}$ ) and core B32 ( $69.8 \text{ kg m}^{-2} \text{ a}^{-1}$ ) equal each other. Finally, at DML07, the two cores from different campaigns also agree: DML9707 from 1997 ( $59.3 \text{ kg m}^{-2} \text{ a}^{-1}$ ) and B31 from 1998 ( $59.8 \text{ kg m}^{-2} \text{ a}^{-1}$ ). These findings show that the small-scale variability of the accumulation rate is compensated for over a period of 35 years.

This first compilation of the spatial distribution of the accumulation rates is based on seven tritium-dated 10 m cores (Oerter and others, 1999) and on 17 DEP- or CFA-dated 30 m firn cores, described in this paper, which gave means for 1960–96 and 1810–1997, respectively (Table 4). To mix both datasets with different time spans seems to be jus-

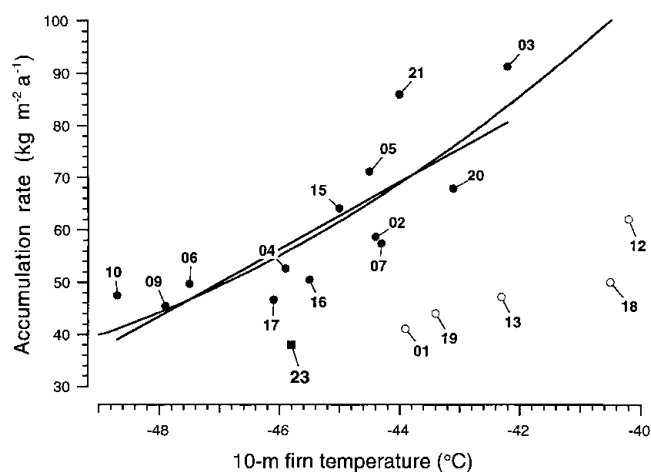


Fig. 7. Relationship between accumulation rate and 10 m firn temperature. The straight line gives the regression line through the data points. The curve represents the fit of a function, which is proportional to the temperature derivative of the mixing ratio, to the data points. The accumulation rates are proportional to the water-vapour loss from a cooling air mass. The data from sites marked by open symbols were omitted in the fitting procedures.

tified for this first approach. According to the stacked record, the 200 year mean equals the mean which results from the tritium dating over the last 35 years, within 5%. The alternative, to take only the mean values over the last 35 years from all cores, would have reduced the number of accumulation values available (five cores are not yet dated on an annual basis) and the accuracy of the accumulation rates, because the Agung eruption is not clearly visible in all DEP profiles.

For compiling the contour map, the dataset was complemented by accumulation values from the Nordic traverse in 1996/97 (Isaksson and others, 1999) to improve the eastern boundary conditions. In addition, south of DML09, the accumulation values of the South Pole–Queen Maud Land Traverse in 1964–68 (Piciotto and others, 1971) were used and, between DML02 and DML05, the accumulation value of  $77 \text{ kg m}^{-2} \text{ a}^{-1}$  reported by Isaksson and others (1996) was included. The spatial interpolation was calculated using a thin-plate spline function (Barrodale and others, 1993), an interpolation tool included in the EASI/PACE software package (all points are given the same weight). The generated accumulation distribution is shown in Figure 6. West, as well as east, of the studied area spots with accumulation rates less than  $45 \text{ kg m}^{-2} \text{ a}^{-1}$  were found. In the middle, mainly eastwards of DML05 along the ice divide, the accumulation rates are  $45\text{--}65 \text{ kg m}^{-2} \text{ a}^{-1}$ . Towards the north, the accumulation rates increase to around  $90 \text{ kg m}^{-2} \text{ a}^{-1}$ , as determined at DML03. The accumulation rate reported by Isaksson and others (1996) causes a southwards-bounded tongue in the pattern. This means that for this location this value is higher than expected from the AWI firn cores alone. How the accumulation rates develop further to the southwest will be revealed by the Swedish–Norwegian work as well as by the British Antarctic Survey 1997/98 field season. Both groups recovered a 130 m core (locations CV and BAS depot in Fig. 1) and shallow firn cores.

#### Relationship between temperature and accumulation rates

The spatial distribution of accumulation rates may reflect

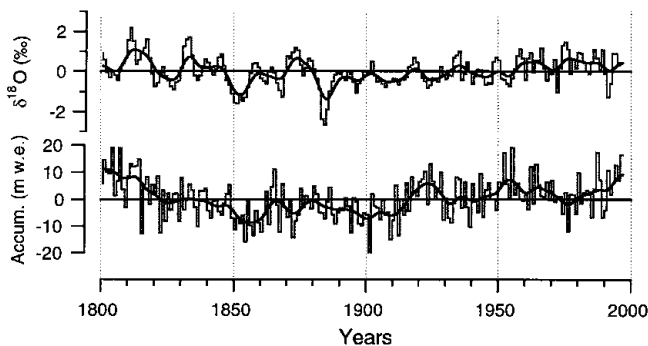


Fig. 8. Composite annually resolved time series of  $\delta^{18}\text{O}$  values (above) and accumulation rates (below). Shown are the deviations of annual values from the 1800–1997 means. The smoothed curve was calculated using a Gaussian low-pass filter over 11 years.

the precipitation field and should be governed by the temperature field. To test, if the accumulation rates and the air temperature are correlated, we used the 10 m firn temperature (Table 1) at the sample sites. This firn temperature stands for the mean annual air temperature over the last few years and is not representative for the last 200 years, but for the correlation only the temperature differences are of interest. Figure 7 displays the accumulation rate and temperature datasets.

At a first step, the accumulation rates and the 10 m temperature in DML were correlated linearly. The relationship becomes significant if the values of the six sites, DML01, DML12, DML13, DML18, DML19 and DML23, are omitted (Fig. 7). All these points (except DML23) are in the west of the plateau. Without them a gradient of  $6.4 \text{ kg m}^{-2} \text{ a}^{-1} \text{ K}^{-1}$  results. With the same accuracy, the data can be approximated by a function proportional to the derivative of the mixing ratio (Fig. 7). That means, the accumulation rates on the DML plateau are strongly correlated with the loss of water vapour from a cooling air mass. With a similar equation, which considers the decrease of the water content with temperature and the temperature gradient, the accumulation rates on the Ronne Ice Shelf could be calculated (Graf and others, 1999). The low accumulation rates at some of the sites in the western part may be due to the trajectories of moist air masses which reach the plateau from the northeast (Noone and others, 1999) or may be caused by katabatic winds, which are stronger in the west than in the central part of Amundsenisen, as indicated by surface roughness.

### Time series of accumulation rates and climate

Oerter and others (1999) investigated ten firn cores recovered in the 1995–97 field seasons. In the meantime, the first stable-isotope data from the 1997/98 cores have also become available. These data include five time series of  $^{18}\text{O}$  content extending to the beginning of the 19th century; the cores are from DML05 (core B32), DML17 (core B33), DML18 (core FB9804), DML15 (core FB9814) and DML14 (core FB9815). The individual series were stacked to a composite record to enhance the signal-to-noise ratio. According to the composite record, the  $\delta^{18}\text{O}$  content decreased in the 19th and increased in 20th century. The increase of the  $\delta^{18}\text{O}$  content in the 20th century (1905–97,  $0.0078 \text{ } \delta^{18}\text{O} - \text{‰ a}^{-1}$ ) is lower

than the decrease during the 19th century (1801–1905:  $-0.0128 \text{ } \delta^{18}\text{O} - \text{‰ a}^{-1}$ ).

Figure 8 shows the composite record of the accumulation rates and that of the  $^{18}\text{O}$  content for the same time interval. In the following only the long-term trend of the composite time series is considered. Visual inspection already shows the similarity of both composite time series. The analysis reveals a positive correlation between  $^{18}\text{O}$  content and accumulation rates with  $r = 0.20$  for the unsmoothed records. The correlation becomes better by smoothing the series with a Gaussian low-pass filter over 11 years, which yields a correlation coefficient of  $r = 0.33$ . This positive cross-correlation is remarkable and makes it probable that the variation both of the accumulation rate and the isotope content are caused by temperature fluctuations. The data are consistent: using the temperature–isotope relationship determined for the Amundsenisen region  $5.5 \pm 0.3 \text{ } \delta^2\text{H} - \text{‰ K}^{-1}$  (Oerter and others, 1999), which corresponds to  $0.69 \pm 0.04 \text{ } \delta^{18}\text{O} - \text{‰ K}^{-1}$ , the composite  $^{18}\text{O}$  record infers a temperature increase of 1.04–1.2 K in the 20th century and a temperature decrease of 1.93–2.26 K in the 19th century. The variation of the accumulation rates is nearly exactly what is expected from these temperature variations. With the empirical relationship between 10 m temperature and accumulation rate on Amundsenisen given above ( $6.4 \pm 1.5 \text{ kg m}^{-2} \text{ a}^{-1} \text{ K}^{-1}$ ), the temperature variations would indicate an increase of the accumulation rate since 1905 of  $6.7\text{--}7.7 \text{ kg m}^{-2} \text{ a}^{-1}$  and a decrease from 1801 to 1905 of  $12.3\text{--}14.5 \text{ kg m}^{-2} \text{ a}^{-1}$ . From the accumulation-rate gradients discussed above nearly the same values follow, for the 20th century an increase of  $6.3\text{--}7.4 \text{ kg m}^{-2} \text{ a}^{-1}$  and for the 19th century a decrease of  $12.9\text{--}13.5 \text{ kg m}^{-2} \text{ a}^{-1}$ . This consistency of the accumulation and isotope data supports the interpretation that temperature changes have caused the variations in the stable-isotope content and accumulation rates over the last two centuries.

### CONCLUSION

Dating the firn cores was done using chemical-constituent data from the DEP and CFA analyses. Very distinct peaks displayed in the DEP and CFA profiles can be assigned to volcanic events and serve as time markers to establish a depth time-scale; this was refined by seasonal signals in the measuring profiles. The eruption of the following volcanoes are well recorded in the firn layers across Amundsenisen: Krakatoa (1883), Tambora (1815), an unknown volcano (1809), Kuwae (1458) and El Chichon (1258). The volcanic origin of the peaks is very probable, but not yet proven by sulphate measurements. The dating is accurate to within one year close to the time markers and may fluctuate between these markers by  $\pm 2$  years. A dating only by stratigraphic means, without known reference horizons, leaves the time series with high ambiguities.

Comparison of the DEP profiles showed that during the past 200 years the relative changes in the accumulation rate were the same at almost all locations. This is also supported by cross-correlation analysis between the individual and composite records. Most pronounced are the different trends in the 19th and 20th centuries. These trends correspond to those in the composite record of the  $^{18}\text{O}$  content. A climatic cause for these trends seems very probable. Both trends can be explained by the same temperature variations. The observed variations of the accumulation rates

are within the limits of natural variability. The values at the end of the 20th century are no higher than at the beginning of the 19th century.

The mean accumulation rates were used to calculate the distribution of the accumulation rates. The resulting pattern is reasonable. The mean accumulation rates can be explained partly by the temperature field.

The DEP profiles and the annual variations within these profiles indicate that the annual layering in the investigated part of Amundsenisen is very regular and that precipitation during all seasons is comparably well conserved in the snow cover. From this point of view, the investigated area of Amundsenisen seems to be favourable as a drill location.

## ACKNOWLEDGEMENTS

We thank A. Ebbeler (AWI) for doing the ECM measurements, H. Rufli (University of Berne) and W.-D. Hermichen, A. Jaeschke and F. Valero-Delgado (AWI) for assistance in the field and cold laboratories at AWI. A. Olfmann and P. Seibel (GSF) as well as G. Meyer and E. Viehoff (AWI) for doing the isotope measurements. Thanks go to all members of the German EPICA traverse in 1997/98 for assisting in the fieldwork.

Financial support by the Deutsche Forschungsgemeinschaft (project Re762/2 and Oel30/3) is gratefully acknowledged. This work is a contribution to the "European Project for Ice Coring in Antarctica" (EPICA), a joint European Science Foundation/European Commission (EC) scientific programme, funded by the EC under the Environment and Climate Programme (1994–98) contract ENV4-CT95-0074 and by national contributions from Belgium, Denmark, France, Germany, Italy, The Netherlands, Norway, Sweden, Switzerland and the United Kingdom. This is EPICA publication No. 6 and AWI publication No. 1664.

## REFERENCES

- Barrodale, L., D. Skea, M. Berkley, R. Kuwahara and R. Poekert. 1993. Warping digital images using thin plate splines. *Pattern Recognition*, **26**(2), 375–376.
- Cole-Dai, J., E. Mosley-Thompson and L. G. Thompson. 1997. Annually resolved Southern Hemisphere volcanic history from two Antarctic ice cores. *J. Geophys. Res.*, **102**(D14), 16,761–16,771.
- Delmas, R. J., S. Kirchner, J. M. Palais and J.-R. Petit. 1992. 1000 years of explosive volcanism recorded at the South Pole. *Tellus*, **44B**(4), 335–350.
- Dome-F Deep Coring Group. 1998. Deep ice-core drilling at Dome Fuji and glaciological studies in east Dronning Maud Land, Antarctica. *Ann. Glaciol.*, **27**, 333–337.
- Gerland, S., H. Oerter, J. Kipfstuhl, F. Wilhelms, H. Miller and W. D. Miners. 1999. Density log of a 181 m long ice core from Berkner Island, Antarctica. *Ann. Glaciol.*, **29**, 215–219.
- Glen, J. W. and J. G. Paren. 1975. The electrical properties of snow and ice. *J. Glaciol.*, **15**(73), 15–38.
- Graf, W., O. Reinwarth, H. Oerter, C. Mayer and A. Lambrecht. 1999. Surface accumulation on Foundation Ice Stream, Antarctica. *Ann. Glaciol.*, **29**, 23–28.
- Hammer, C. U. 1980. Acidity of polar ice cores in relation to absolute dating, past volcanism, and radio-echoes. *J. Glaciol.*, **25**(93), 359–372.
- Isaksson, E., W. Karlén, N. Gundestrup, P. Mayewski, S. Whitlow and M. Twickler. 1996. A century of accumulation and temperature changes in Dronning Maud Land, Antarctica. *J. Geophys. Res.*, **101**(D3), 7085–7094.
- Isaksson, E., M. R. van den Broeke, J.-G. Winther, L. Karlöf, J. F. Pinglot and N. Gundestrup. 1999. Accumulation and proxy-temperature variability in Dronning Maud Land, Antarctica, determined from shallow firn cores. *Ann. Glaciol.*, **29**, 17–22.
- Langway, C. C., Jr, H. B. Clausen and C. U. Hammer. 1988. An inter-hemispheric volcanic time-marker in ice cores from Greenland and Antarctica. *Ann. Glaciol.*, **10**, 102–108.
- Langway, C. C., Jr, K. Osada, H. B. Clausen, C. U. Hammer, H. Shoji and A. Mitani. 1994. New chemical stratigraphy over the last millennium for Byrd Station, Antarctica. *Tellus*, **46B**(1), 40–51.
- Langway, C. C., Jr, K. Osada, H. B. Clausen, C. U. Hammer and H. Shoji. 1995. A 10-century comparison of prominent bipolar volcanic events in ice cores. *J. Geophys. Res.*, **100**(D8), 16,241–16,247.
- Legrand, M. R. and S. Kirchner. 1990. Origins and variations of nitrate in south polar precipitation. *J. Geophys. Res.*, **95**(D4), 3493–3507.
- Looyenga, M. 1965. Dielectric constants of heterogeneous mixture. *Physica*, **31**(3), 401–406.
- Moore, J. C. and J. G. Paren. 1987. A new technique for dielectric logging of Antarctic ice cores. *J. Phys. (Paris)*, **48**, Colloq. C1, 155–160. (Supplément au 3)
- Moore, J. C., H. Narita and N. Maeno. 1991. A continuous 770-year record of volcanic activity from East Antarctica. *J. Geophys. Res.*, **96**(D9), 17,353–17,359.
- Newhall, C. G. and S. Self. 1982. The volcanic explosivity index (VEI): an estimate of explosive magnitude for historical volcanism. *J. Geophys. Res.*, **87**(C2), 1231–1238.
- Noone, D., J. Turner and R. Mulvaney. 1999. Atmospheric signals and characteristics of accumulation in Dronning Maud Land, Antarctica. *J. Geophys. Res.*, **104**(D16), 19,191–19,211.
- Oerter, H., W. Graf, F. Wilhelms, A. Minikin and H. Miller. 1999. Accumulation studies on Amundsenisen, Dronning Maud Land, by means of tritium, dielectric profiling and stable-isotope measurements: first results from the 1995–96 and 1996–97 field seasons. *Ann. Glaciol.*, **29**, 1–9.
- Palais, J. M., S. Kirchner and R. J. Delmas. 1990. Identification of some global volcanic horizons by major element analysis of fine ash in Antarctic ice. *Ann. Glaciol.*, **14**, 216–220.
- Palais, J. M., S. Germani and G. A. Zielinski. 1992. Inter-hemispheric transport of volcanic ash from a 1259 A.D. volcanic eruption to the Greenland and Antarctic ice sheets. *Geophys. Res. Lett.*, **19**(8), 801–804.
- Picciotto, E., G. Crozaz and W. de Breuck. 1971. Accumulation on the South Pole–Queen Maud Land traverse, 1964–1968. In Crary, A. P., ed. *Antarctic snow and ice studies II*. Washington, DC, American Geophysical Union, 257–315. (Antarctic Research Series 16)
- Sigg, A., K. Fuhrer, M. Anklin, T. Staffelbach and D. Zurmühle. 1994. A continuous analysis technique for trace species in ice cores. *Environ. Sci. Technol.*, **28**(2), 204–209.
- Wagenbach, D. and 7 others. 1998. Sea-salt aerosol in coastal Antarctic regions. *J. Geophys. Res.*, **103**(D9), 10,961–10,974.
- Wilhelms, F. 1996. Leitfähigkeits- und Dichtemessung an Eisbohrkernen. *Ber. Polarforsch.* 191.
- Wilhelms, F., J. Kipfstuhl, H. Miller, K. Heinloth and J. Firestone. 1998. Precise dielectric profiling of ice cores: a new device with improved guarding and its theory. *J. Glaciol.*, **44**(146), 171–174.